THE EFFECTS OF POROSITY ON LUNAR CRATER FORMATION AND THE TRANSITION FROM COMPLEX CRATER TO PEAK RING BASIN MORPHOLOGY. C. Milbury[1] , B. C. Johnson[1] , H. J. Melosh[1], D. M. Blair, and G. S. Collins[2], [1]Department of Earth, Atmospheric, and Planetary Science, Purdue University, 550 Stadium Mall Drive, Hampton Hall, Room 3233, West Lafayette, IN 47907, [2]Earth Science and Engineering Department, Imperial College London, Exhibition Road, London SW7 2BP, UK. (cmilbury@purdue.edu).

Introduction: The observed transition from simple to complex crater morphology is driven by gravitational collapse of the transient crater. The mechanism that causes the transition from complex to peak-ring crater morphology, however, is somewhat contentious. There are two dominant models that have been proposed to explain this transition in crater morphology: the central peak collapse model [1, 2] and the nested melt cavity model [3, 4]. Both models predict the observed morphological features and depth to diameter ratios. By calculating peak and peak ring volumes, Bray et al. [5] showed that the data tend to support peak-ring formation by collapse of the central peak.

Melosh [6] was the first to put forward the idea of acoustic fluidization (AF), which is the temporary behavior of fractured rock as a viscous fluid. It is triggered by intense, short-wavelength vibrations within the target and it occurs mostly within the crater collapse phase of the impact process. Wünnemann & Ivanov [7] carried out simulations using the AF model to match the observed depth to diameter ratios over a range of crater sizes for the Moon, Earth, and Venus.

In this study, we systematically investigate this change in crater morphology using the iSALE hydrocode and varying the AF parameters over a broad range of values. We will identify where melt is produced and calculate the melt volume so these can be compared with the nested melt cavity model predictions. We investigate the effects that porosity and dilatancy have on the final morphological features of the craters. The results are then compared to topographic data and data from NASA's dual Gravity Recovery And Interior Laboratory (GRAIL) spacecraft.

Methodology: We use the following model parameters in our simulations: an equation of state for granite in the crust and for dunite in the mantle, an impact velocity of 17 km/s, a surface gravity of 1.6249 m/s^2, and a thermal gradient of 5 K/km. We use the strength parameters for gabbroic anorthosite for the crust and dunite for the mantle from Potter et al. [8].

We systematically vary the AF parameters, γ_β and γ_η [7], to understand how they affect crater morphology. γ_β is a scaling factor related to the decay time and controls the amount of time the target is subject to AF. The decay time is given by the equation $T_{dec} = \gamma_\beta \left(\frac{r}{c_s}\right)$, where r is the impactor radius, and c_s is the speed of sound. γ_η is a scaling parameter related to the viscosity by the equation $\eta = \gamma_\eta c_s r \rho$, where η is the kinematic viscosity, and ρ is the density.

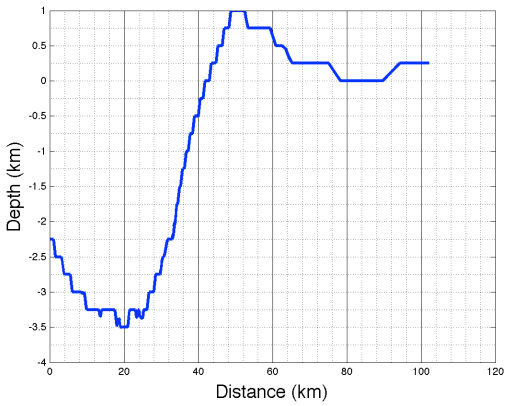

Figure 1. Plot of topography for a complex crater that matches the characteristics of Copernicus crater well. This plot is axisymmetric, with the axis of symmetry shown at the left edge of the figure.

For each model run, the crater depth, diameter, and central peak height and width are compared to those determined by Kalynn et al. [9] for lunar complex craters using topographic data. The impactor size is increased to produce basin-sized craters. These are compared with specific craters on the Moon, and the gravity signatures associated with these craters are calculated from our models and compared to gravity data from GRAIL [10].

Results and Discussion: Figure 1 shows a profile of the topography of a crater 700 s after impact with a 6 km dunite impactor. γ_β is 350, and γ_η is 0.102 and 1.02 for the crust and mantle, respectively. This simulation produced a crater that is 98 [100] km in diameter, 4.5 [4.4] km deep, a central peak height of 1.25 [1.27] km, and a central peak width of 20 [20] km, where the values in brackets are from [9] for comparison. Within the 250 m resolution of the simulation, this is in excellent agreement with the observations for a crater in the mare.

We calculated the free-air and Bouguer gravity anomalies for the simulation shown in Figure 1 (see Figure 2). Comparison of Figures 2 and 3 shows that the free-air anomaly matches the GRAIL free-air gravity anomaly well. Unfortnately, there is a large feature in the Bouguer gravity (probably the mantle uplift of an ancient and previously unrecognized much larger

crater) that obscures much of the anomaly associated with Copernicus crater, however, the part that is not obscured is in good agreement with the Bouguer anomaly for the simulation.

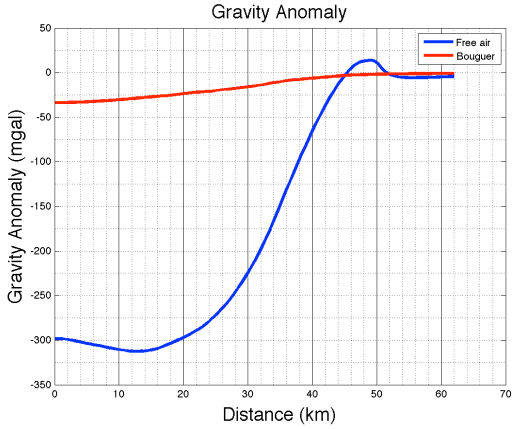

Figure 2. Plot of the free-air (blue) and Bouguer (red) gravity anomalies calculated from the crater model shown in Fig. 1.

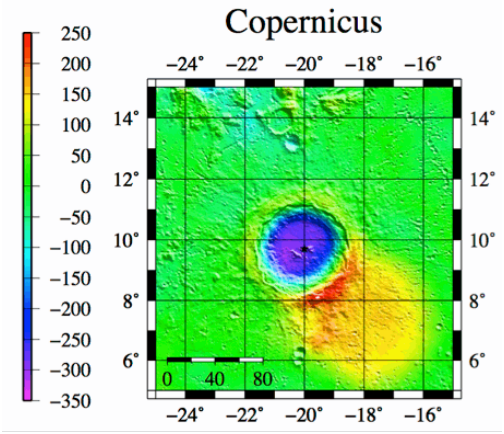

Figure 3. Plot of the free-air gravity anomaly (mgal) of Copernicus crater.

The same AF parameters that reproduce the complex craters, produce peak-ring basins that are deeper than observed basins. GRAIL revealed that the lunar subsurface is very porous [11], which has a large effect on the gravity signature, so we have begun to incorporate porosity into our models. We find that when we model a porous crust (with a porosity of 13.6%), we have to decrease γ_η and the viscosity of fluidized material shocked to a given shock pressure by two orders of magnitude due to the attenuation of the shock wave in a porous target. This is illustrated in Figure 4, where it is clear the inclusion of porosity dampens the shock wave, and therefore requires a lower effective viscosity than previous models of AF-medieated crater collapse. At the distance near the final crater rim (40 km) and a depth of 10 km, the peak shock pressure is ~2 orders of magnitude different larger for the non-porous/porous case. Figure 5 shows a plot of the topography for one such simulation. Including porosity produces a crater that is ~1 km deeper than one with a non-porous target.

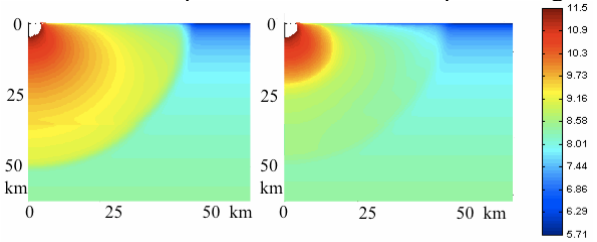

Figure 4. Contour plots in the x-y plane of the peak shock pressure after 12 s at the position of the tracers after 0.5 after the impact for non (porous) left (right) targets. The color bar is in log(Pa).

Our simulations also show that the melt produced by the impact is in a layer that lines the transient crater, contrary to the nested melt cavity model where the melt is concentrated in a region below the center of the transient crater. Similar to previous hydrocode studies, we find that peak ring morphological features are a result of collapse of the central uplift.

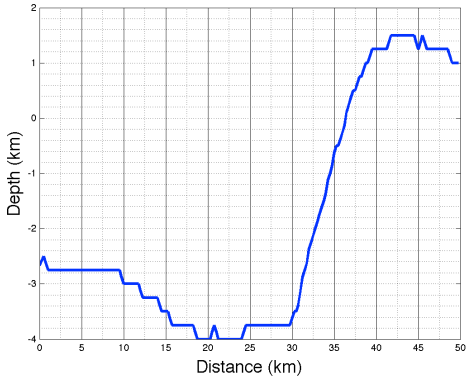

Figure 5. Topographic profile for a run with porosity included, where γ_η and γ_β are 10^{-3} and 300, respectively.

Summary and Future Work: We are able to reproduce complex craters that match the observed morphological features and observed gravity signature of complex craters well. In order to better fit the peak-ring basin morphology and gravity signature, we are incorporating dilatancy (bulking resulting from shearing during crater formation) into our models.

References: [1] Morgan, J. V. et al (2000) *EPSL, 183*, 347-354. [2] Collins, G. S. et al. (2002) *Icarus, 157*, 24-33. [3] Head J. W. et al (2010) *GRL, 37*, L02203. [4] Baker D. M. et al (2011a) *Icarus, 214*, 377–393. [5] Bray V. J. et al. (2012) *GRL, 39*, L21201. [6] Melosh (1979) *JGR, 84*, 7513-7520. [7] Wünnemann K. and Ivanov B. A. (2003) *PSS, 51*, 831-845. [8] Potter, R. W. K. et al. (2013) *JGR, 118*, 963-979. [9] Kalynn J. et al. (2013) *GRL, 40*, 38-42. [10] Zuber M. T. et al. (2012), *Science* doi: 10.1126/science.1231507. [11] Wieczorek M. A. et al. (2012) *Science*, doi: 10.1126/science.1231530.